IRAQI
Academic Scientific Journals

Kirkuk Journal of Engineering Science
Electronic ISSN: 3106-5597

journal homepage: https://kirkukjes.com/index.php/kjes

Seepage Analysis Through Earthen Dam by Artificial- Neural-Networks (ANNs): Duhok Dam as a Case Study

Derin Rauf Saber *, Chelang A. Arslan
Department of Civil Engineering, University of Kirkuk, Kirkuk, Iraq

A B S T R A C T

An earthen dam is a structure made of soil particles that are bonded together and compacted in layers using mechanical methods. depend on their weight to combat forces such as sliding & overturning. Seepage passage during earth dam is the principal cause of collapse owing to erosion, scouring, and piping. The passage of water during soil can result in the displacement of the particles. Ongoing motion induces erosion. This study depends on Artificial Neural Networks (ANN) for estimation seepage in Duhok dam, utilizing measured upstream water level and flow rate, as well as piezometric head measurements from four distinct parts of the dam structure. The findings indicated excellent model efficacy. Artificial Neural Network models necessitate less field data, rendering them advantageous for dam safety evaluations, providing insights into their relative efficacy in forecasting seepage in earthen dams under diverse scenarios. The results were derived from established statistical metrics R^2, MAE, MAPE and E-NASH. This research concluded that many ANNs has excellent forecasting capabilities.

A R T I C L E I N F O

Keywords:
Earth dam
Multiple ANN
Seepage
Duhok dam

Article history:
Received: 17 Dec. 2024
Received in revised from: 30 Mar. 2024
Accepted: 06 April 2025
Published: 01 Sep. 2025

*Corresponding author
derinrauf238@gmail.com

1. Introduction

Population Dams are constructions utilized primarily for water storage, electricity generation, and irrigation. Dams are primarily categorized into four types based on construction materials and design: gravity dams, buttress dams, arch dams, and embankment dams. Embankment dams are categorized into two types: homogeneous and nonhomogeneous dams. Non-homogeneous dams consist of various components, each significantly impacting the dam's performance, stability, and other design elements independently [1]. More than 85% of all constructed dams are embankment dams[2].

An earthen dam is a structure made of soil particles that are bonded together and compacted in layers using mechanical methods. Earth dams often possess a trapezoidal form featuring a wide base. It was engineered as a non-overflow segment featuring an independent spillway. In the design of an earth dam, the base, abutments, and embankment must be regarded as a cohesive unit. In this type of dam, the soil's shear strength guarantees its stability [3]. Earth dams can be split into four principal types: homogeneous earth dams, zoned earth dams, earthfill dams with core walls, and concrete-faced earth dams [4]. Salem, et al. [3] conducted experimental and numerical studies on seepage through the body of an earth dam, both with and without an interior core. Various models have been analyzed utilizing the GEOSTUDIO (2012) software concerning SEEP/W and SLOPE/W. SEEP/W was utilized for seepage calculations, whilst SLOPE/W was employed for slope stability studies. SLOPE/W a subprogram of Geo-Slope software was utilized by Zedan , et al. in conjunction with SEEP/W software to determine the factor of safety of the upstream slip surface through drawdown conditions for Khasa Chai dam [5].

Erosion in earthen constructions transpires when seepage pressures surpass the soil's resistance, which is contingent upon cohesion, particle interlinking, soil weight as well as downstream protection. As seepage in earthen constructions is irregular, erosion is exacerbated in regions with considerable seepage [6]. The seepage lane within the dam's structure is

crucial for the planning and execution of economically and technically viable remedial stability measures, as excessive seepage may jeopardize the dam's stability [7]. Hutchison [7] created a model for the Texas Instruments TI-59 programmable calculator to estimate reservoir seepage. The dam seepage model delineates flow through and beneath the dam by positing that, the interface between the dam and its foundation constitutes a streamline. The employed algorithm is founded on Darcy's law, Dupuit's postulates, and Bear's hydraulic methodology. Mohammadi et al. [8] progressed three evolutionary algorithms: Shuffled Complex Evolution (SCE), Simulated Annealing (SA), and Genetic Algorithm (GA) to optimize the geometry of the Birjand Hesar Sangi earth dam core, focusing on seepage integration, hydraulic gradient, and stability safety factor constraints.

Artificial- Neural- Networks (ANN) are fundamental components utilized in machine-learning. Owing to their remarkable self-learning and self-adapting abilities, they have been thoroughly researched and effectively employed to address complex real-world challenges [9]. The ANN can be characterized as a fundamental engineering principle within the domain of artificial intelligence. This network is engineered by emulating the human nervous system. An ANN is a network of interconnected nodes or neurons. These nodes can retain experiential information and render it accessible for utilization. These nodes represent the fundamental units of information processing. The training of ANN encompasses various methodologies and applications, including Perceptron, Back-propagation, Self-Organizing Map (SOM) and Delta [10].

A multitude of neural- networks have been created and examined in recent decades. This encompasses self-organizing networked neurons, the Hopfield networks, the radial basis- function networks, Boltzmann's machine, mean field theory machines, and multiple-layer perceptron's, (MLPs) [11]. A literature study conducted by Shahin et al. in 2001 indicates that artificial neural networks (ANNs) have been effectively employed to solve some geotechnical engineering challenges [12]. In this research MLP was used.

MLP neural networks comprise units organized in layers. Each layer consists of nodes, and in the fully interconnected networks, each node is linked to every node in the subsequent layers. Each MLP comprises at least three layers, which include an input layer, various hidden layers, and a layer for the output [11]. The research provided by Arslan, et al. predicts the discharge coefficient of cylinder-shaped crest weirs utilizing various diameters, angles of inclination, and bed slopes. Also, the adaptive-neuro-fuzzy-inference-system (ANFIS) and multilayer perceptron (MLP) models were employed utilizing 143 laboratory test [13]. In 2001,Manry, et al. introduced three techniques that assist academics in applying the MLP to signals processing challenges [14]. Shahin et al. [15] employed artificial-neural-networks to achieve enhanced accuracy in settlement predictions. A substantial database of empirically measured settlements is utilized to create and validate the model of ANN. The anticipated settlements derived from the use of ANNs are juxtaposed with the values forecasted by three widely employed conventional approaches. This study investigates seepage in Duhok earth-fill dams because the study of seepage helps to ensure the sustainability of the operation of earth dams and reduce the risks associated with them.

2. Methodology

2.1. Case Study

The Duhok Dam is a substantial earth-fill dam featuring a central clay core and a gravel shell, situated on the Rubar Duhok (2) kilometers north of Duhok city in northwestern Iraq, near the Turkish border [16], between the latitudes 36°52′35″ N– 36°54′21″ N, and the longitudes 42°59′51″ E– 43°00′40″ E as shown in Figure 1. It was formed in 1988 [17]. Duhok Dam is situated in the southwestern section of what is called Be khair Anticline [18]. The parameters for the dam and reservoir are a height of 60.5 meters, a crest length of 740 meters, and a width of 9 meters. The reservoir has a capacity of 52 million m^3 and a total area ranging from 1,670,000 m^2 to 2,800,000 m^2 [19]. Both the main and coffer dams are constructed as earth-fill structures including a central clay core, flanked by a layer of filter material on each side, and protected by a shell of sand and gravel [20], as shown in Figure 2 [21]. The primary objective of the dam was to irrigate the agricultural regions inside Duhok city and its surrounding territories up to Summel city via a tunnel. Currently, the reservoir area of the dam serves to supply Duhok city with water and has also developed into a tourist destination [17].

2.2. Artificial-Neural-Network

A multi-artificial neural network model was developed in this study to estimate seepage in the Duhok Dam. Utilized data sets were employed to train and to test the generated model. They included water levels in the piezometers, as well as the water level at the upstream side of the dam and the outflow rate. MATLAB, along with the Neural-Network- Toolbox, was utilized for model development. The upstream water level and outflow rate were the input variables, while the piezometer water levels were the outputs (targets) in the ANN model. Figure 3 shows the depiction of a multi-layered artificial neural network architecture accompanied by a neuron illustration [22]. The model employed a feed-forward-neural- network, utilizing a sigmoid activation function and the Levenberg-Marquardt back propagation algorithm for learning. The back propagation algorithm is the most renowned method for training ANNs. Back propagation involves exploring an error surface (error as a function of artificial neural network weights) by gradient descent to identify points with minimal error. Iteration in back propagation has two phases: a forward pass to generate a solution and a backward pass to propagate the computed error for weight adjustment [23]. Various scenarios were simulated using distinct layer activation functions and inputs. The situations were simulated utilizing the available toolbox options, with parameters modified by using the (nftool) function in MATLAB. The artificial -neural -network model comprised three layers (input, hidden, output) layers. The input layer had two neurons, and the output layer also comprised two neurons. The quantity of neurons in the hidden layer was ascertained by trial and error. This methodology was executed across four designated portions, each containing two piezometers, as depicted in the accompanying diagram-(4): illustrating their placements [20].

The numbers of hidden layers and neurons within the hidden layer can be configured in the toolbox. All input and output data were normalized to the range of (0-1) utilizing Excel. The research employed water level data from eight piezometers, comprising a total of 355 data sets gathered between July 27, 2004, and September 9, 2024. Out of them, 283 sets were allocated for training the network, while 72 sets were designated for testing and validating the model. The network was trained using a predetermined learning rate.

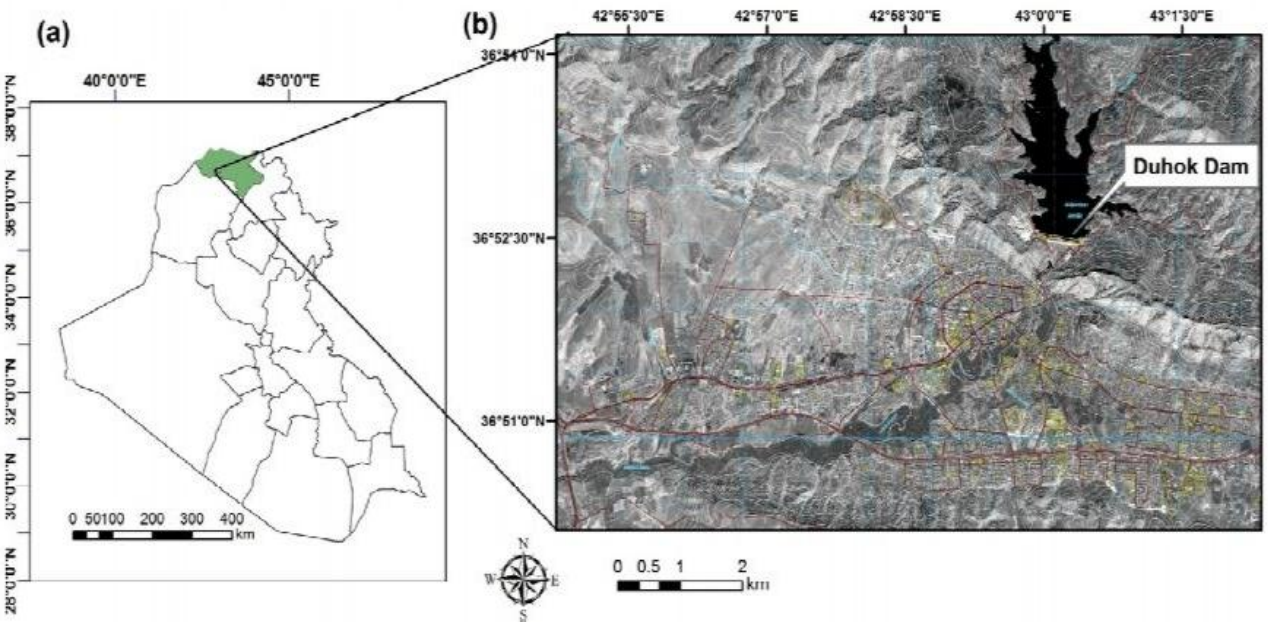

Fig.1. Duhok dam location [17].

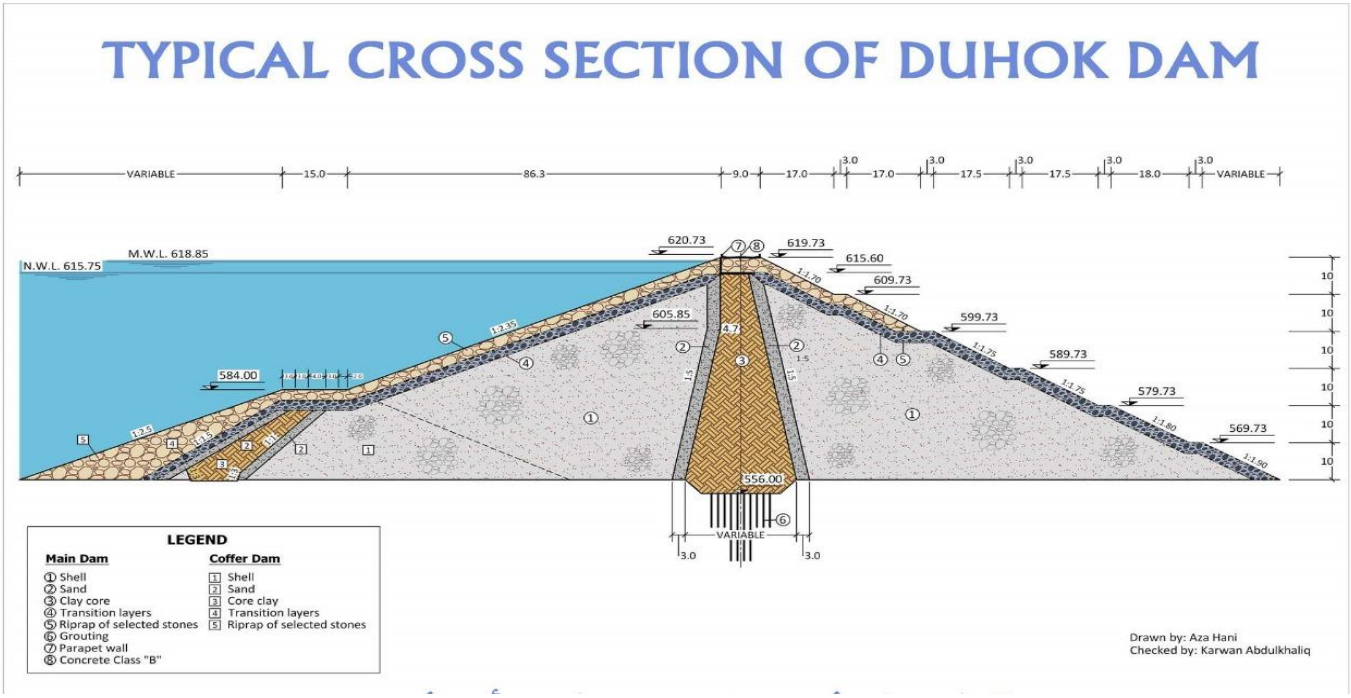

Fig. 2. Typical section of Duhok dam [21].

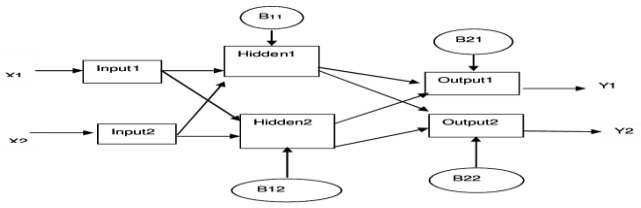

Fig. 3. Depiction of a multi-layered artificial neural network architecture accompanied by a neuron illustration [22].

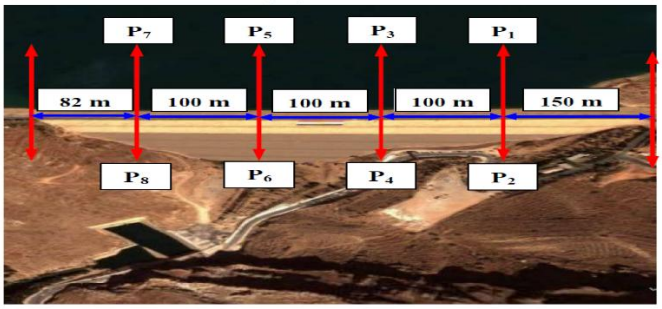

Fig. 4. The locations of the piezometers in Duhok dam [20].

3. Results and Discussion

3.1. Standardization Process

Normalization:

It is the procedure of normalizing the data to a certain range, such as between (0 - 1) or between (-1 - +1). Normalization becomes crucial if there are significant disparities in the ranges of certain variables. It is derived using the formula shown for data standardization between (0-1):

$$X_n = \frac{X_j - X_{\min}}{X_{\max} - X_{\min}} \quad (1)$$

Denormalization:

This step should be performed if normalization is used. For instance, to deformalize the data from the range of (0-1), the following equation can be employed:

$$X_j = [X_n(X_{\max} - X_{\min})]X_{\min} \quad (2)$$

X_n represents the normalized data,

X_j denotes the measured or denormalized data,

$X_{\min}$ and $X_{\max}$ refer to the identical values utilized in the normalization procedure [24].

Statistical Parameters:

Four prominent statistical criteria were applied to evaluate and examine the performance of the employed models during separate training and testing phases. These parameters include Measure of Correlation (R^2) , Mean- Absolute- Error (MAE) ,Mean -Absolute- Percentage- Error (MAPE), Nash-Sutcliffe Efficiency (E-Nash):

$$R^2 = \frac{[\sum_{j=1}^{n}(xj - \overline{xj})(Ej - \overline{Ej})]^2}{\sum_{j=1}^{n}(xj - \overline{xj})^2 \sum_{j=1}^{n}(Ej - \overline{Ej})^2} \quad (3)$$

$$\text{MAE} = \frac{1}{n}\sum_{j=1}^{n}|x_j - E_j| \quad (4)$$

$$\text{MAPE} = \frac{1}{n}\sum_{j=1}^{n}\left|\frac{x_j - E_j}{x_j}\right| \quad (5)$$

$$\text{E} - \text{NASH} = 1 - \frac{\sum_{j=1}^{n}(Xj - Ej)^2}{\sum_{j=1}^{n}(Xj - \bar{E}_j)^2} \quad (6)$$

where:

Xj : real value,

$\overline{X_j}$: mean real value,

Ej : estimated value,

$\bar{E}_j$: mean estimated value [25]

3.2. Results

The upstream water levels and flow rate, and the piezometric head values at different locations, were divided into two separate sets: once for training and another for testing. About 80 %, of the data was assigned to the training set; while the other 20%, was given to the test set. This distribution corresponds to approximately 283 values for the training phase and 72 values for the testing phase throughout the complete series. The input nodes represented both upstream water level and flow rates. Simultaneously, the output node was tasked with representing each individual piezometric head, a procedure executed for each piezometer within every specified section. A three-layer Feed-Forward- Back -Propagation- network was utilized, with training conducted using the Levenberg Marquardt reduction algorithm. A Tangent Sigmoid transfer function was employed for the hidden layer, whilst a linear transfer function was applied to the output layer. Table 1 presents the values of validation parameters for both the training and test periods.

3.3. Discussion

Depending on the value of the measure of correlation R^2, which is significant as it assesses the quality of the match. If its value approaches (1) The value of the slope of the regression line is almost one, and its point of intercept is approximately zero. The network training was completed effectively. The results in the table above shown that Multiple- Artificial- Neural-Networks presented excellent performance. A succinct comparative can be derived through looking at the various plotted series for the training and test phases. Figures 5 to 20 illustrate the comparative performance for each piezometric heads.

Table 1. Statistical parameter values for the ANN model for the piezometers in four section.

Name of Model		No of hidden neuron	TRAIN				TEST			
			R^2	MAE	MAPE	E-Nash	R^2	MAE	MAPE	E-Nash
Section (1)	P1	12	0.988	0.3557	0.0588	0.9881	0.992	0.2852	0.0470	0.9921
	P2	12	0.929	0.3864	0.0645	0.9284	0.954	0.3137	0.0523	0.9531
Section (2)	P3	10	0.980	0.4923	0.0813	0.9788	0.985	0.5113	0.0846	0.9848
	P4	10	0.963	0.4134	0.0691	0.9628	0.978	0.3748	0.0626	0.9769
Section (3)	P5	10	0.994	0.2554	0.0421	0.9936	0.997	0.2223	0.0367	0.9968
	P6	10	0.971	0.3390	0.0568	0.9712	0.989	0.2379	0.0398	0.9884
Section (4)	P7	9	0.996	0.2626	0.0433	0.9956	0.992	0.2596	0.0428	0.9910
	P8	9	0.962	0.3173	0.0533	0.9622	0.902	0.3411	0.0574	0.8982

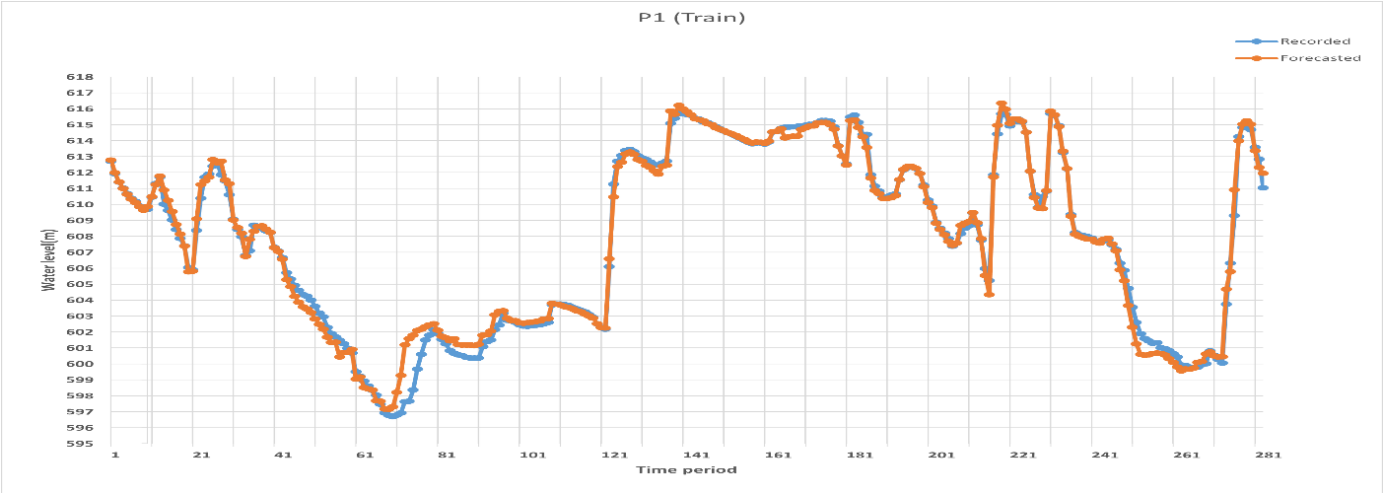

Fig. 5. Recorded and forecasted water levels during piezometer P1 during training period.

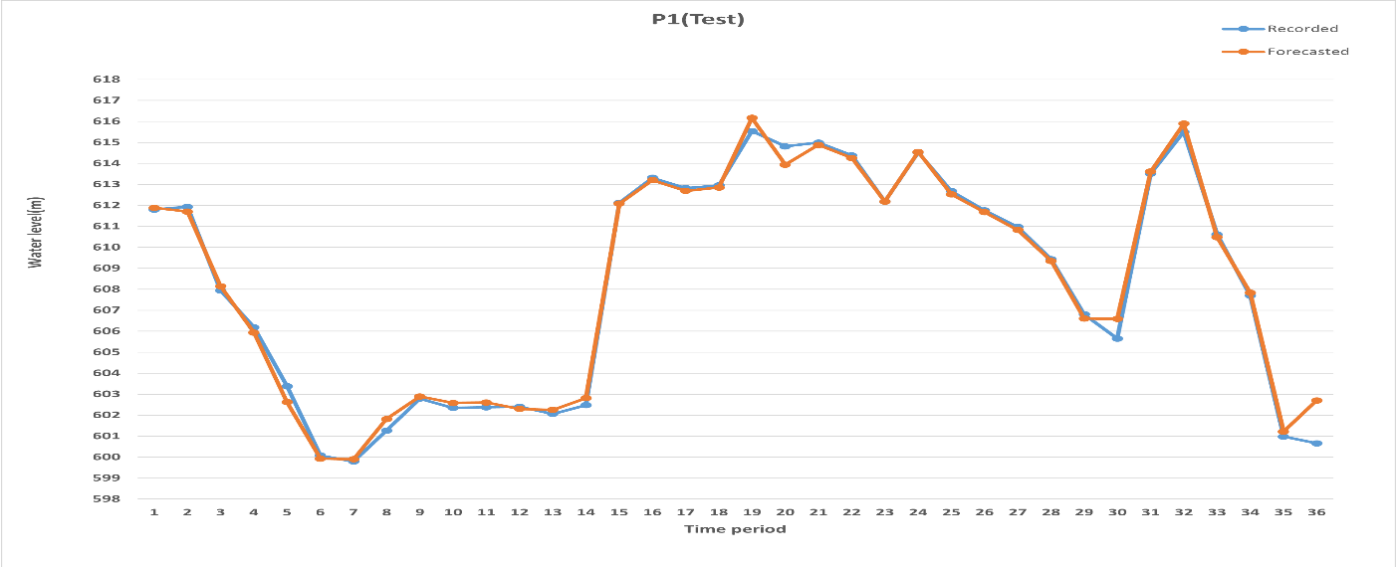

Fig. 6. Recorded and forecasted water levels during piezometer P1during test period.

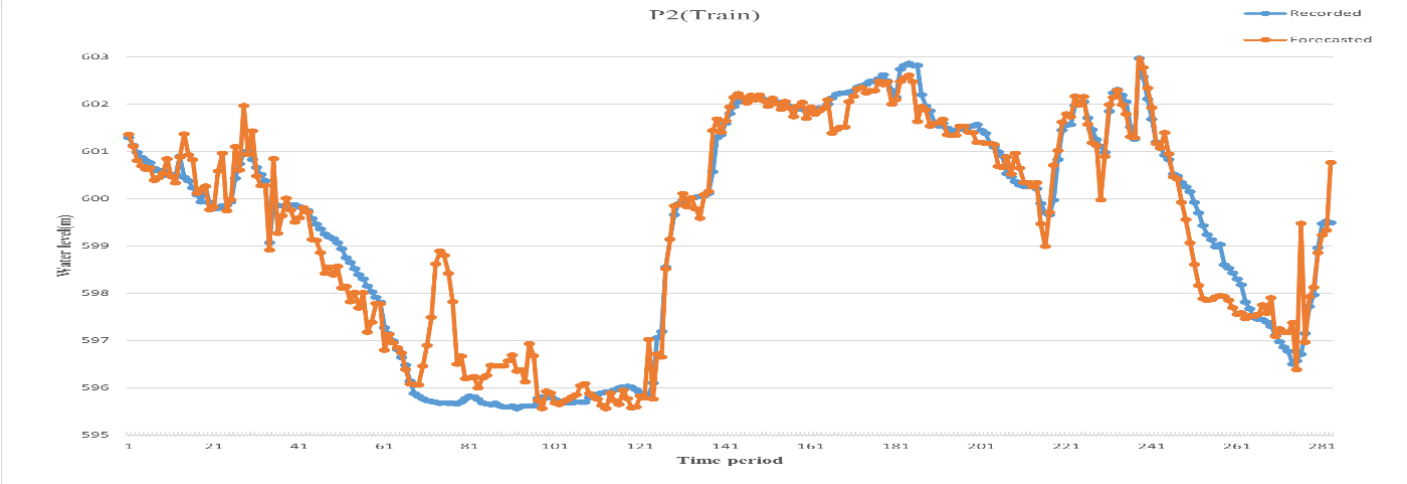

Fig. 7. Recorded and forecasted water level during piezometer P2 during training period.

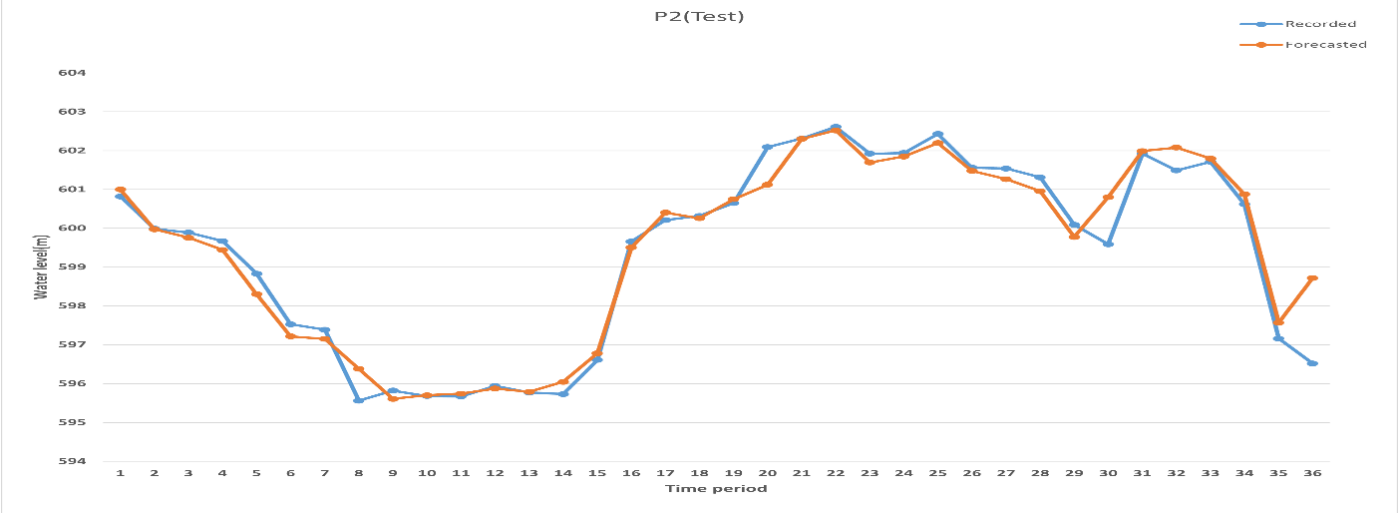

Fig. 8. Recorded and forecasted water level during piezometer P2 during test period

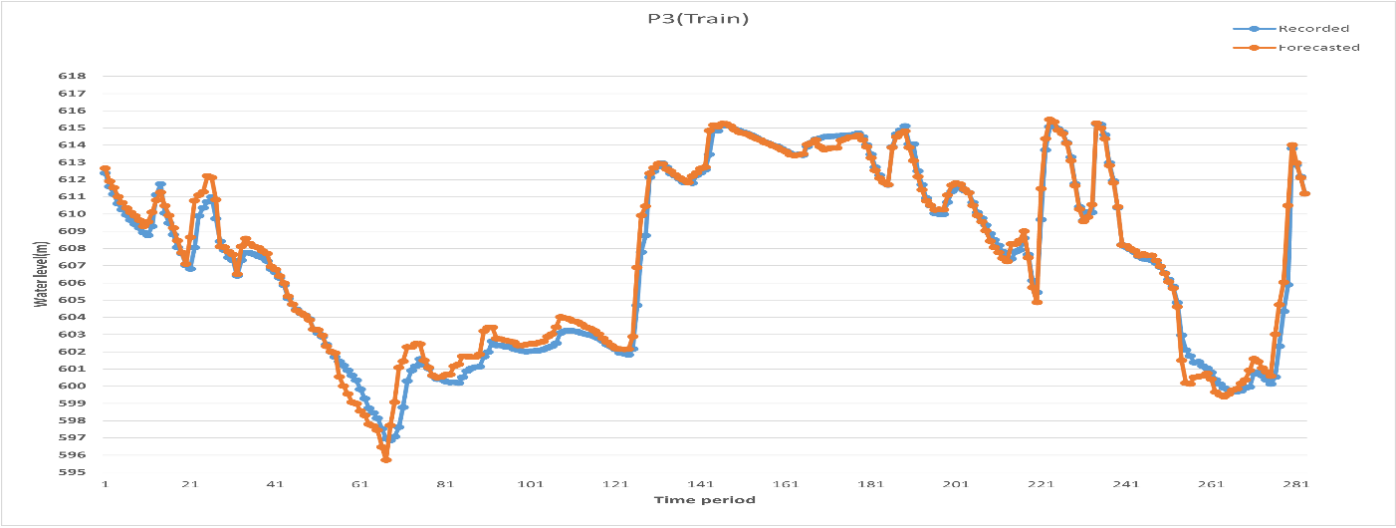

Fig. 9. Recorded and forecasted water level during piezometer P3 during training period.

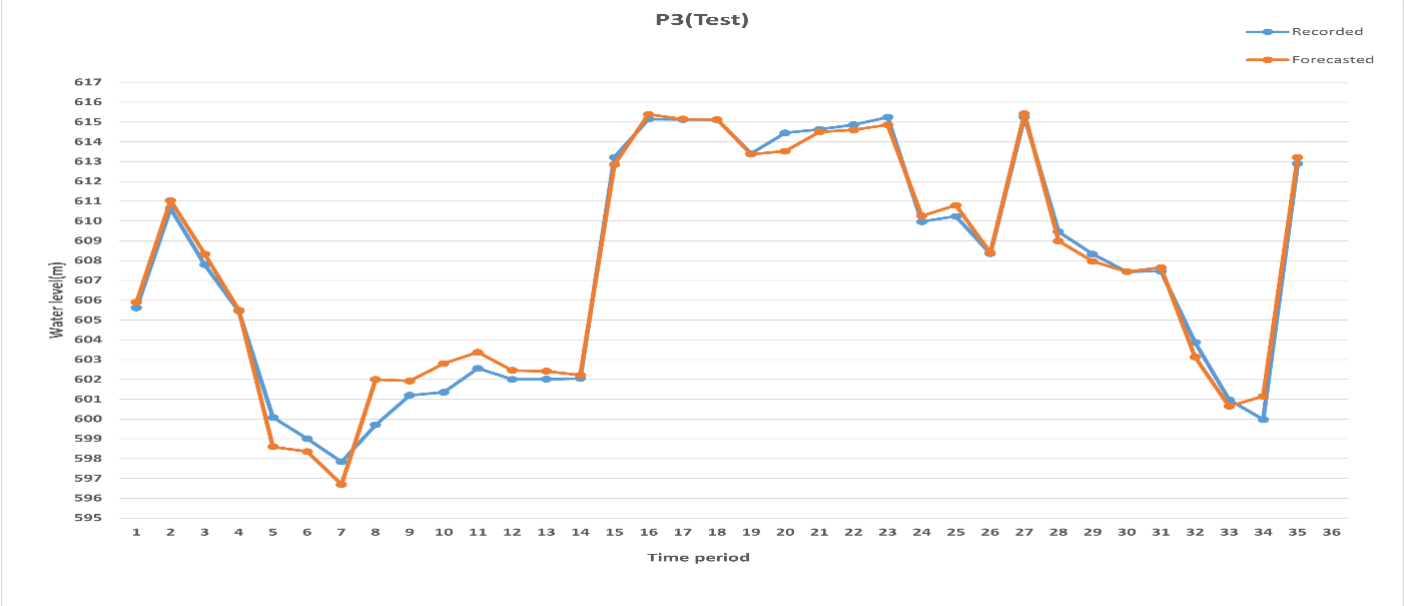

Fig. 10. Recorded and forecasted water level during piezometer P3 during test period.

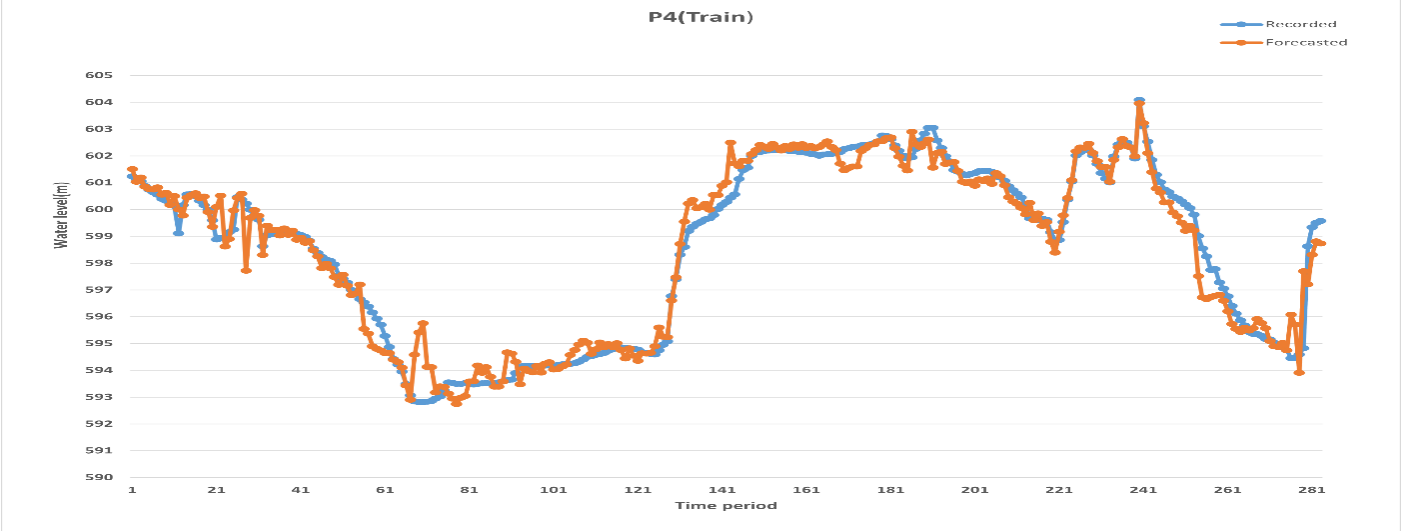

Fig. 11. Recorded and forecasted water level during piezometer P4 during training period.

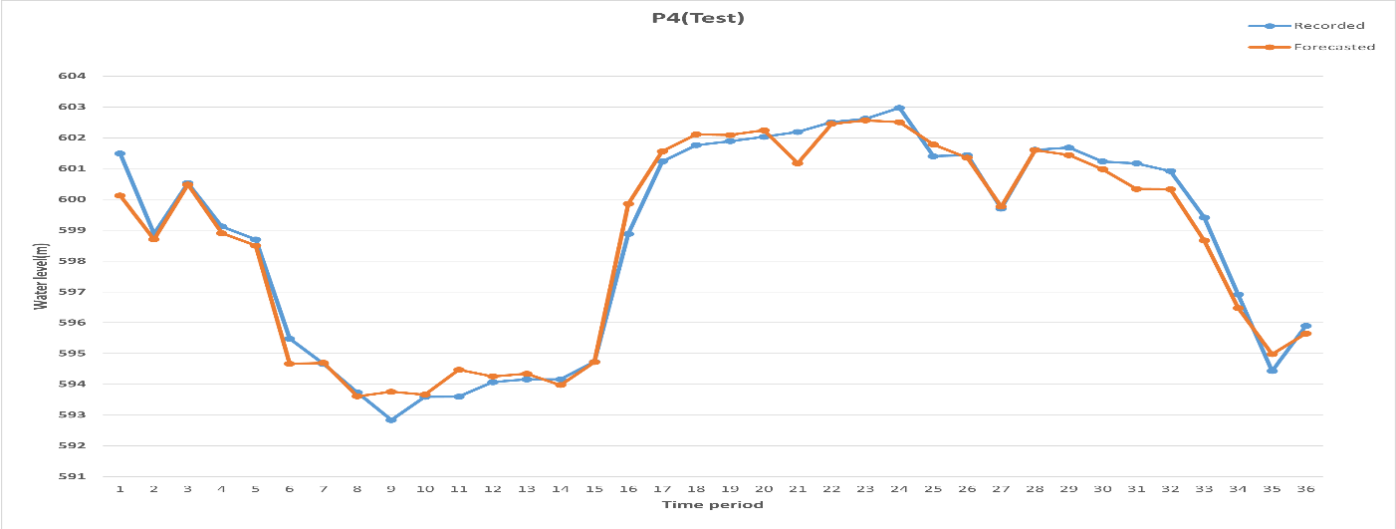

Fig. 12. Recorded and forecasted water level during piezometer P4 during test period.

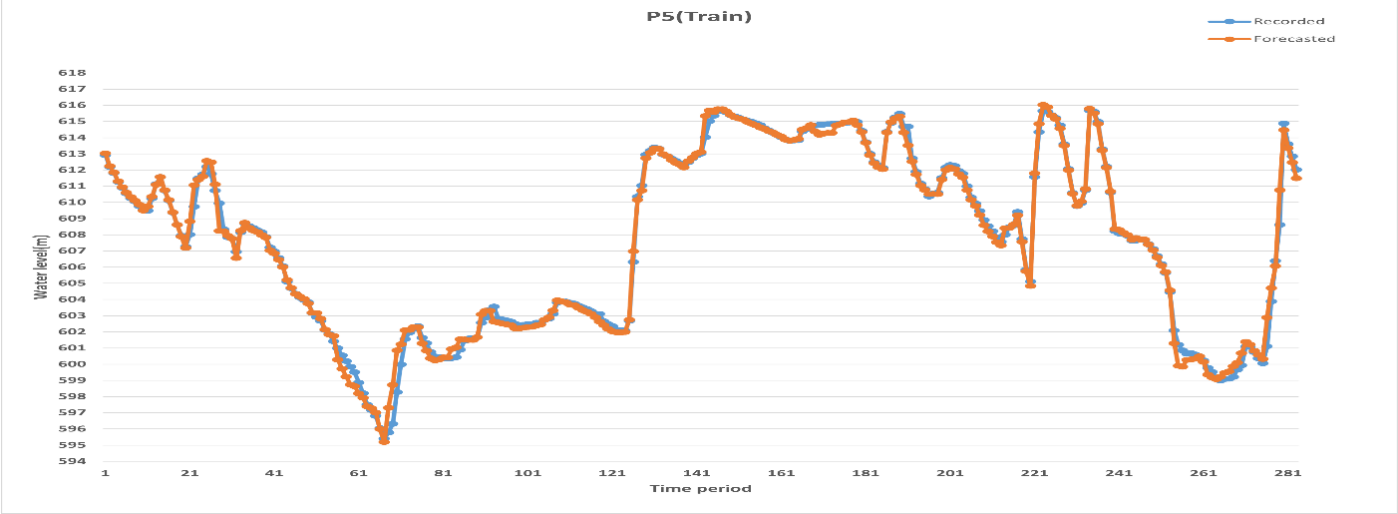

Fig. 13. Recorded and forecasted water level during piezometer P5 during training period.

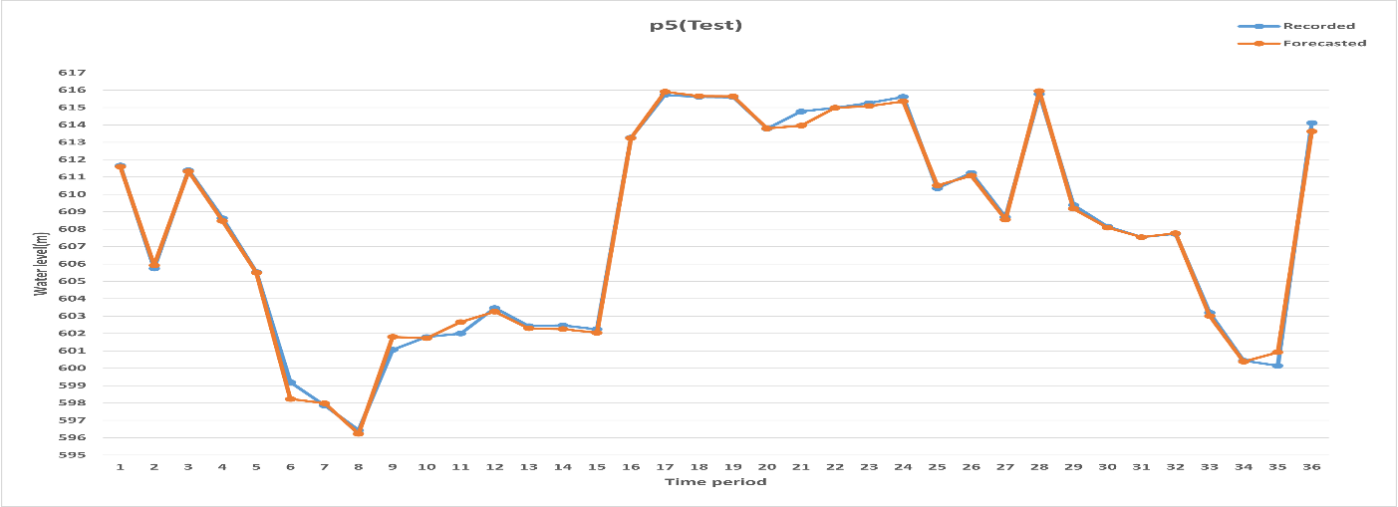

Fig. 14. Recorded and forecasted water level during piezometer P5 during test period.

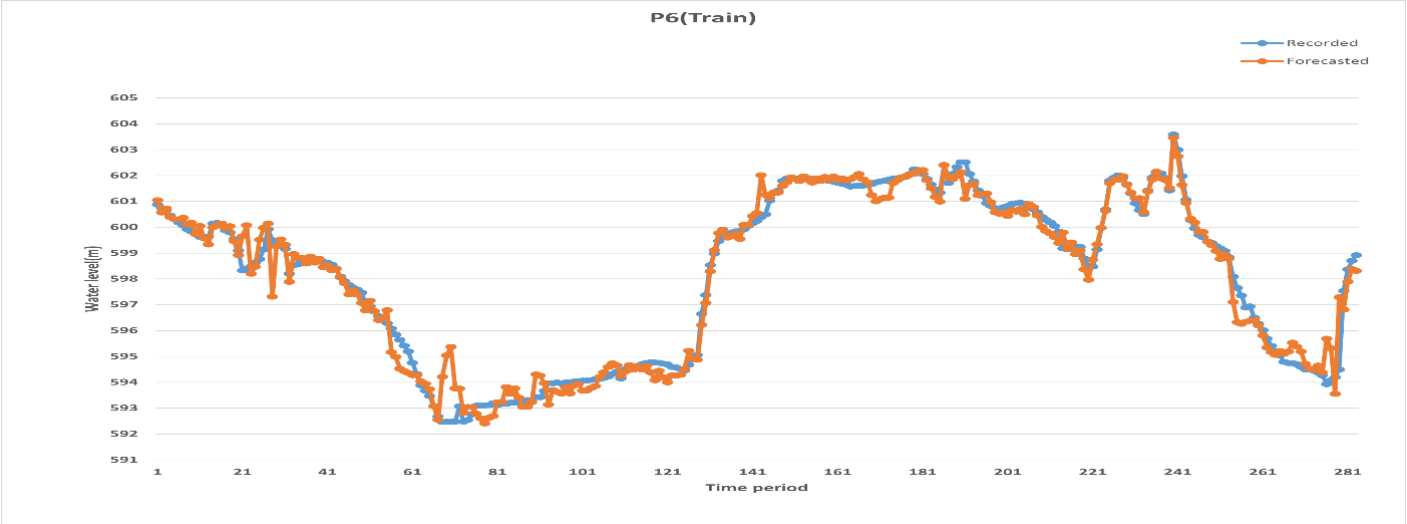

Fig. 15. Recorded and forecasted water level during piezometer P6 during training period.

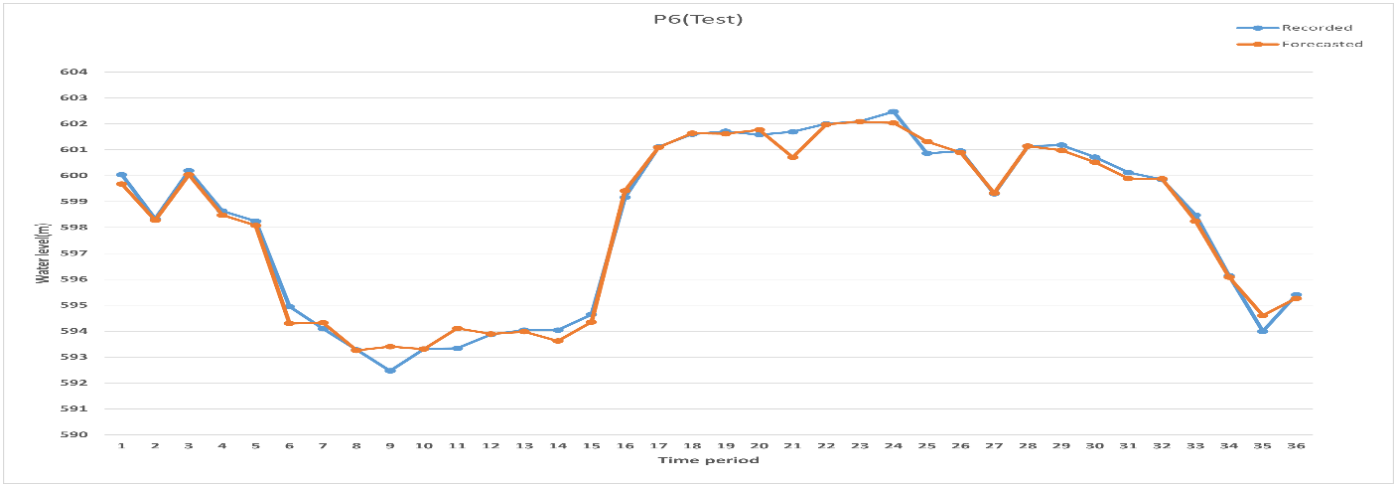

Fig. 16. Recorded and forecasted water level during piezometer P6 during test period.

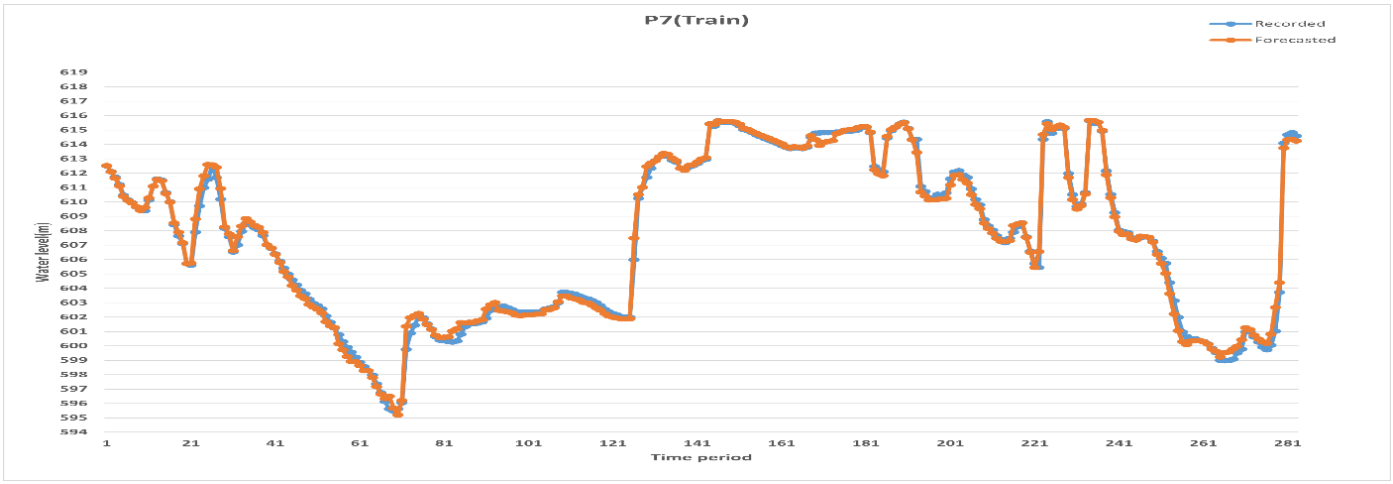

Fig. 17. Recorded and forecasted water level during piezometer P7 during training period.

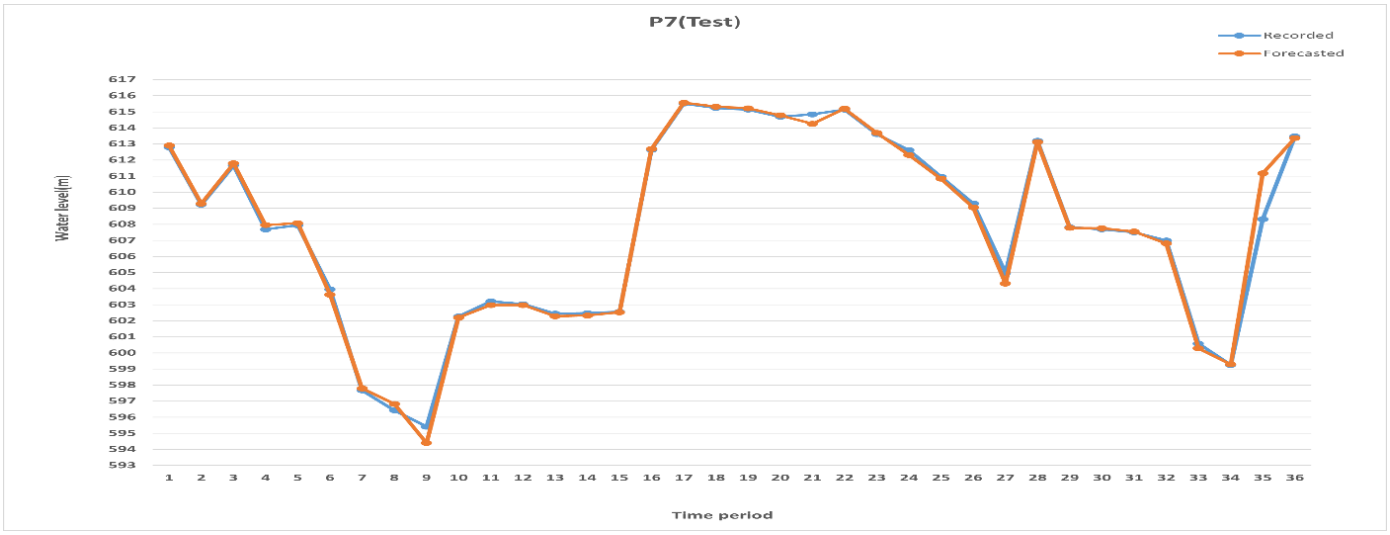

Fig. 18. Recorded and forecasted water level during piezometer P7 during test period.

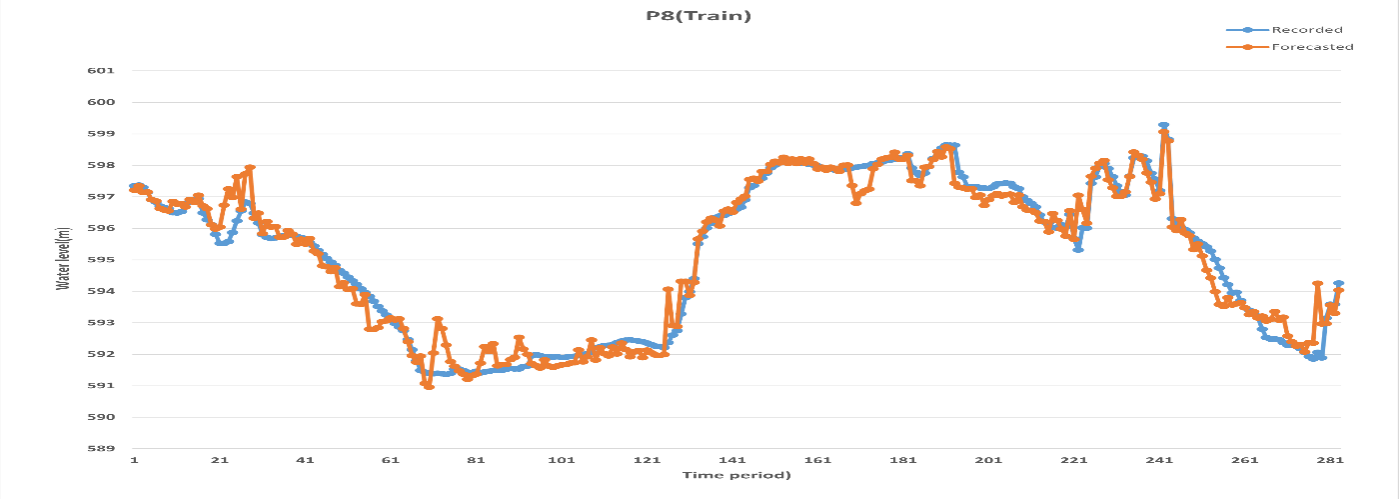

Fig. 19. Recorded and forecasted water level during piezometer P8 during training period.

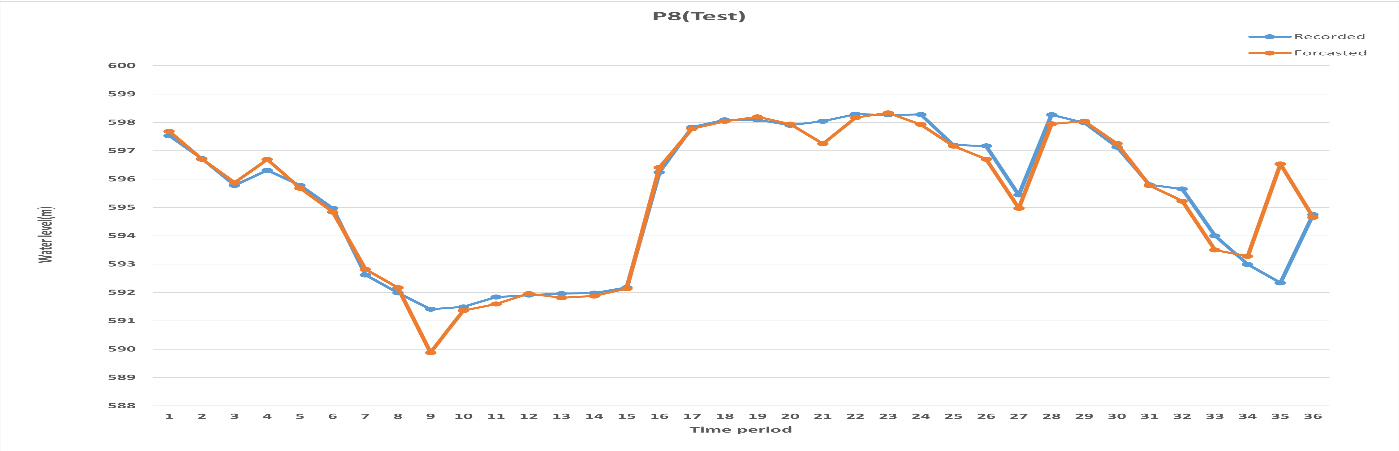

Fig. 20. Recorded and forecasted water level during piezometer P8 during test period.

4. Conclusions

The artificial neural network is an efficient and accessible model for identifying patterns between input and output data, provided it is supplied with adequate observed field data. The results show that Multiple- Artificial- Neural- Networks presented excellent performance. A succinct comparative can be derived through looking at the various plotted series for the training and test phases. Figures 5 to 20 illustrate the comparative performance for each piezometric heads.

As stated earlier, all models were calibrated and validated using data collected from piezometers strategically located along the length of the Dohuk dam, which is designated for seepage monitoring. It was capable of identify the correlation between the upper reservoir water level and the flow rate and the piezometers water levels. Consequently, it is feasible to anticipate the trajectory of the seepage path within the earth-fill dam. However, it is acknowledged that the ANNs operates as a black box model. Thus, this facilitates the development and implementation of both technically and economically effective corrective stability measures. It is helpful engineers tasked with dam safety in addressing unnatural seepage through an earth-fill dam under diverse conditions.

The data utilized to substantiate this analysis was supplied by the Ministry of Agriculture and Water Resources in Kurdistan region- Iraq, the general directorate of dams and reservoirs, the private Dohuk dam project management.

Acknowledgements

The authors would like to thank the College of Engineering at the University of Kirkuk for supporting this work. The Duhok dam management for providing field data of the Duhok dam. It is very appreciated by the authors.

References

[1] Ersayin D. Studying seepage in a body of earth-fill dam by Artificial Neural Networks. (M.Sc. Thesis), İzmir Institute of Technology: Turkey, 2006.

[2] Kiraa M.S., Zeidan B., Nasr A.M., Heza Y.B. Storage earth dam failure due to liquefaction caused by earthquakes. *The Open Civil Engineering Journal*, vol. 17: pp. e1-8, 2023. Doi: 10.2174/0118741495260786230926063103

[3] Salem M.N., Eldeeb H.M., Nofal S.A. Analysis of seepage through earth dams with internal core. *International*

Journal of Engineering Research, vol. 8(1): pp. 768-777, 2019. Doi: 10.17577/IJERTV8IS080168

[4] Zhang L.M., Y. X., Jia J.S. Analysis of earth dam failures: A database approach. *Georisk: Assessment and Management of Risk for Engineered Systems and Geohazards*, vol. 3(3): pp. 184-189, 2009, Doi: 10.1080/17499510902831759

[5] Zedan A.J., Faris M.R., Abdulsattar A.A. Slope stability of an earth dam during drawdown conditions (KHASA-CHAI dam) as a case study. *International Journal of Engineering and Technology*, vol. 7(37): pp. 17-21, 2018. Doi: 10.14419/ijet.v7i4.37.23605

[6] Flores-Berrones R., Lopez-Acosta N.P. *Internal erosion due to water flow through earth dams and earth structures*: InTech, 2011.

[7] Hutchison W.R. Earth dam seepage analysis with a programmable calculator. (M.Sc. Thesis), University of Arizona: Arizona, USA, 1983.

[8] Mohammadi M., Barani G., Ghaderi K., Haghighatandish S. Optimization of earth dams clay core dimensions using evolutionary algorithms. *European Journal of Experimental Biology*, vol. 3(3): pp. 350-361, 2013.

[9] Aksu G., Güzeller C.O., Eser M.T. The effect of the normalization method used in different sample sizes on the success of artificial neural network model. *International journal of assessment tools in education*, vol. 6(2): pp. 170-192, 2019. Doi: 10.21449/ijate.479404

[10] Arslan C.A., Kayis E. Weather forecasting models using Neural Networks and Adaptive Neuro Fuzzy inference for two case studies at houston, Texas and dallas States. *Journal of Asian Scientific Research*, vol. 8(1): pp. 1-12, 2018. Doi: 10.18488/journal.2.2018.81.1.12

[11] Delashmit W.H., Manry M.T. Recent developments in multilayer perceptron neural networks. in *The Seventh Annual Memphis Area Engineering and Science Conference, MAESC*. pp. 248-253, 2005.

[12] Shahin M.A., Jaksa M.B., Maier H.R. Artificial neural network applications in geotechnical engineering. *Australian Geomechanics*, vol. 36(1): pp. 49-62, 2001,

[13] Chelang A., Abdul-Karim A., Ismael A. Prediction of discharge coefficient for cylindrical weirs using adaptive neuro fuzzy inference system ANFIS and multilayer neural networks MLP. *International Journal of Applied Engineering Research*, vol. 13(9): pp. 7042-7051, 2018.

[14] Manry M.T., Chandrasekaran H., Hsieh C.-H., *Signal processing using the multilayer perceptron*, in *Handbook of Neural Network Signal Processing*. 1st edition, 2018, CRC Press: Florida, USA.

[15] Shahin M.A., Maier H.R., Jaksa M.B. Predicting settlement of shallow foundations using neural networks. *Journal of geotechnical and geoenvironmental engineering*, vol. 128(9): pp. 785-793, 2002. Doi: 10.1061/(ASCE)1090-0241(2002)128:9(785)

[16] Mohammed R. The impact of the man activity in Duhok dam watershed on the future of Duhok dam lake North-Iraq. in *1st International Applied Geological Congress, Islamic Azad University-Mashad Branch, Iran*, pp. 26-28, 2010.

[17] Mustafa Y.T., Noori M.J. Satellite remote sensing and geographic information systems (GIS) to assess changes in the water level in the Duhok dam. *International Journal of Water Resources and Environmental Engineering*, vol. 5(6): pp. 351-359, 2013. Doi: 10.5897/IJWREE2012.0402

[18] Hamdon A.N., Zand R.K., Qubaa A.R., Ali S.H. Geomorphological Analysis of Duhok Dam Site Using Remote Sensing Data. *Iraqi National Journal of Earth Sciences*, vol. 24(1): pp. 1-15, 2024. Doi: 10.33899/earth.2023.139763.1073

[19] Al-Talib S.A., Al-Jawadi A.S., Al-Sanjari A.S.A. Impact of Gercus formation erosion and rock sliding on Duhok dam reservoir–Northern Iraq. *Iraqi Journal of Science*, vol.: pp. 1562-1569, 2021. Doi: 10.24996/ijs.2021.62.5.19

[20] Ismaeel K.S., Noori B.M. Evaluation of seepage and stability of Duhok Dam. *Al-Rafidain Engineering Journal*, vol. 19(1): pp. 42-58, 2011. Doi: 10.33899/rengj.2011.27885

[21] Management D. D. P. Typical section of Duhok dam.

[22] Salehi M., Mansoury A. An evaluation of Iranian banking system credit risk: Neural network and logistic regression approach. *International Journal of the Physical Sciences*, vol. 6(25): pp. 6082-6090, 2011.

[23] Basheer I.A., Hajmeer M. Artificial neural networks: fundamentals, computing, design, and application. Journal of Microbiological Methods, vol. 43(1): pp. 3-31, 2000. Doi: 10.1016/S0167-7012(00)00201-3

[24] Ali P.J.M., Faraj R.H., Koya E., Ali P.J.M., Faraj R.H., *Data normalization and standardization: a technical report*. Learn Technical Report, 2014. pp. 1-6, Doi: 10.13140/RG.2.2.28948.04489

[25] Arslan C.A., Buyukyildiz M. Development of multisite streamflow generation models. *Fresenius Environmental Bulletin*, vol. 25(5): pp. 1502-1512, 2016.